

## Research Article

# Experimental Research on the Effective Utilization of Remaining Oil Based on the Microfluidic Flat Model

Bin Chen <sup>1</sup>, Hai Huang,<sup>1</sup> Le Qu,<sup>1</sup> Qingqing Li,<sup>2</sup> Hongxuan Ge,<sup>3</sup> and Baiqiang Li<sup>4</sup>

<sup>1</sup>Shaanxi Key Lab of Petroleum Accumulation Geology, Xi'an Shiyu University, Xi'an, China 710065

<sup>2</sup>No. 5 Oil Production Plant, Changqing Oilfield Company, PetroChina, Xi'an, China 710200

<sup>3</sup>Research Institute of Shaanxi Yanchang Petroleum (Group) Co., Ltd., Xi'an, China 710075

<sup>4</sup>School of Resources and Environmental Engineering, Hefei University of Technology, Hefei, China 230009

Correspondence should be addressed to Bin Chen; chenbinoil@xsyu.edu.cn

Received 17 March 2022; Accepted 25 May 2022; Published 24 June 2022

Academic Editor: Zhehui Jin

Copyright © 2022 Bin Chen et al. This is an open access article distributed under the Creative Commons Attribution License, which permits unrestricted use, distribution, and reproduction in any medium, provided the original work is properly cited.

Using the micro model plus full-information scanning video, it can vividly and intuitively reproduce the fluid movement during the oil, gas, and water displacement process and the microscopic remaining oil morphology and distribution after the water flooding is completed. Based on the microfluidic flat plate model experiment, this paper discusses the microresidue comprehensively for the specific development well pattern (inverse seven-point well pattern), well type, and fracture occurrence morphology (horizontal fracture) produced by fracturing, taking into account the comparative displacement method, the law of effective use of oil. The research results show that the effect of nitrogen flooding and foam flooding in horizontal fractured conventional wells is better than that of water flooding. The remaining oil after nitrogen flooding and foam flooding is mainly columnar and plug; the remaining oil of water flooding is mainly striped and networked. And the remaining oil saturation is high (72.2%). The main reason for this type of remaining oil is that there is still a large amount of contiguous remaining oil that has not been used; the horizontal fracture horizontal well has the best nitrogen flooding effect, and the remaining oil saturation is low (25.48%), the remaining oil form after nitrogen flooding is mainly striped, the remaining oil content of the other types is low, and the remaining oil form after water flooding is mainly columnar and net.

## 1. Introduction

Water flooding is the main means of oil field development in my country. After years of water flooding development, most of my country's oil fields have entered a period of ultrahigh water cut. Improving the development effect in the high water-cut period is of great significance to the further increase of oil production in water flooding reservoirs [1, 2]. The simulation pore model water drive experiment is an effective method to study the microscopic seepage mechanism [3, 4]. Its biggest advantage is its strong visibility and can simulate various water drive environments at the same time. Many scholars at home and abroad have used the microscopic visualization model to simulate the microscopic motion state of oil and water and then study the distribution of the remaining oil, mainly the real sandstone microdisplacement experimental research represented by

the fluid displacement team of Northwestern University and the tight oil research of China University of Petroleum. The team's flat plate simulation study of the oil-water movement law in the high water-cut period has perfected and developed the remaining oil research theory [5]. Based on the microfluidic flat plate model experiment, this paper discusses the microresidue comprehensively for the specific development well pattern (inverse seven-point well pattern), well type, and fracture occurrence morphology (horizontal fracture) produced by fracturing, taking into account the comparative displacement method [6], the law of effective use of oil. The laser-etched glass model is used to characterize the actual pore structure, well pattern layout, fracture distribution, and development well type of the actual formation. The microfluidic pump is used to simulate the distribution of remaining oil after different displacement methods, and the microscopic remaining oil characteristic parameters are

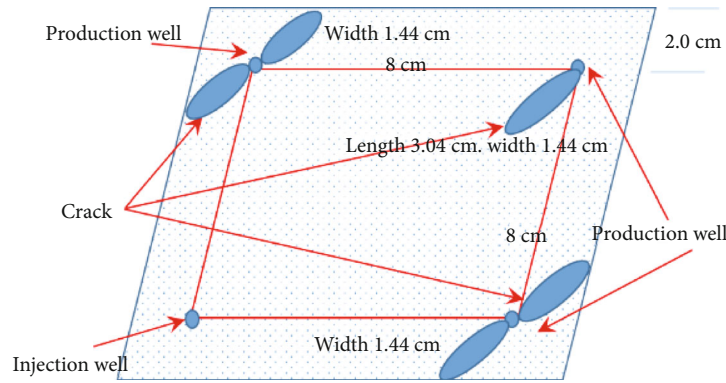


FIGURE 1: Schematic diagram of the visual model of horizontal fractures in conventional wells.

established. The quantitative characterization method uses “number of pores and throats occupied by microscopic remaining oil,” “shape factor,” “oil-rock contact ratio,” and “Euler number” as characteristic parameters to classify and identify microscopic remaining oil and perform quantitative statistics [7]. Furthermore, the occurrence state of microscopic remaining oil in the displacement process is studied, and then, the law of effective production of remaining oil is determined (Liang et al. 2019; [8, 9]).

## 2. Experimental Model

**2.1. Experimental Model Processing.** The geological conditions of the oil reservoir in the study area of this paper are special. The Chang 6 reservoir is the target layer for development. Some oil reservoirs have horizontal fractures or low-angle fractures after fracturing. The statistics of the core analysis data show that the average porosity is 8.35%, and the permeability is the largest. The average permeability is  $0.56 \times 10^{-3} \mu\text{m}^2$ . The microscopic model can intuitively reproduce the oil, gas, and water displacement process of the underground reservoir. In this paper, scan slices of the CT pore structure of the long 6-layer core in the Guoqi area of the Ordos Basin are selected [10, 11]. Laser etching and then sintering the cover glass at high temperature to make a simulated pore model were done. The sample size of the flat model used in this experiment is  $12 \text{ cm} \times 12 \text{ cm}$ , the thickness is about 0.6 mm, the pressure capacity is 0.2–0.3 MPa, the normal pressure temperature resistance is about  $100^\circ\text{C}$ , and the pressurized temperature resistance is about  $80^\circ\text{C}$ . The etching depth is  $30 \mu\text{m}$ , and the lower limit of the actual model pore diameter is  $50 \mu\text{m}$ . Drill holes at the marked position to simulate production and injection wellheads. The diameter of the wellhead is 1.6 mm. Due to the limitations of model materials and surface modification effects, the wettability of the microfluidic model cannot be consistent with the real situation of the core, which hinders the use of microscopic displacement experimental results to guide the field development practice of oil and gas fields [12–16].

**2.2. Microfluidic Flat Panel Design.** According to the actual well spacing and fracture distribution, the conventional well flat model well spacing is 8 cm, the horizontal fracture half-length is 3.04 cm, and the fracture ellipse minor axis length is

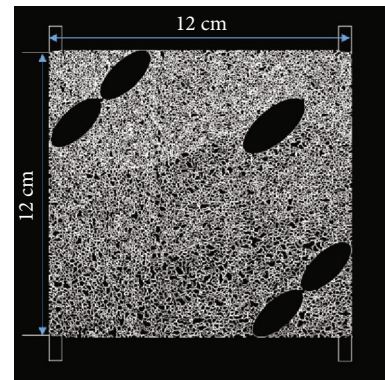


FIGURE 2: Design drawing of horizontal fracture lithography model in conventional wells.

1.44 cm. Fracture strike direction is  $\text{NE } 51.3^\circ$ ; horizontal well flat model horizontal well section length is 6 cm, horizontal fracture half-length is 0.88 cm, short fracture half-length is 0.58 cm, short axis fracture width is 0.2 cm, horizontal well inner diameter is 1.397 mm, fracture is distributed on the two wings of the horizontal well, and the fractures are perpendicular to the horizontal well section. The schematic diagram of the microfluidic flat plate model of conventional wells and horizontal wells used in the experiment is shown in Figures 1–4.

## 3. Microscopic Model Experiment System

- (1) Vacuum system: use a vacuum pressure pump to vacuum the model, exhaust the air in the pores of the model, and minimize the experimental error caused by the gas during the experiment
- (2) Pressurization system: use air compressor to pressurize and digital pressure meter to measure pressure (Microfluidic Precision Pressure Pump-OB1)
- (3) Microscopic observation system: Nikon stereo microscope is mainly used, equipped with digital camera and video system. In the experiment, you can observe various phenomena in real time and take pictures or video at the same time, so as to observe and record important phenomena in real time

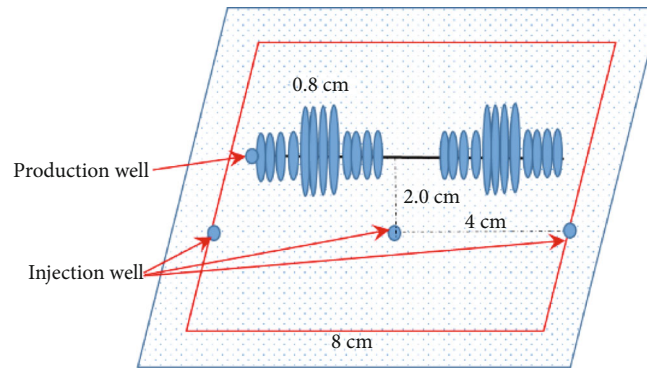


FIGURE 3: Schematic diagram of the visual model of horizontal wells and horizontal fractures.

- (4) Image acquisition system: the system is equipped with a high-resolution camera and camera, which can collect and transmit video signals to a computer (Figure 5)

#### 4. Experiments and Image Analysis Methods

**4.1. Experimental Materials.** The experiment water is deionized water (with dye methyl blue), the experiment oil viscosity is 4 mPa·s no. 5 white oil (with red dye), the oil-water interfacial tension is 63.77 mN/m, and the experiment gas is high-purity nitrogen; the experimental foaming agent is 0.3%YFG802 + 0.05% polyacrylamide, which can effectively reduce the viscosity of crude oil, adjust the water-oil mobility ratio, prevent sticky fingers and water channeling, and increase the swept area. The micro model is made of glass, including two heterogeneous models of horizontal fractured conventional well type and horizontal fractured horizontal well type. The total flow area is 12 cm × 12 cm. The reagents used to repeatedly flush the model before replacing the displacement medium are propanol and deionized water.

The original porosity of the slab is 31.20%, and the average pore diameter is 164.6 μm by the image pore method. The permeability of the slab is  $3296.7 \times 10^{-3} \mu\text{m}^2$  calculated by using the Guccini equation.

#### 4.2. Experimental Procedure

- (1) Vacuum the model and saturate it with water. The experiment was carried out in a constant temperature environment. First, use a vacuum system to extract the air in the plate to prevent the air in the blind ends of the pores or dead pores from affecting the accuracy of the experiment. The vacuuming time lasts for 48 h, and the pressure of the vacuum gauge is -0.1 MPa (Figures 6(a) and 6(c)). In the vacuum state (pressure of -0.1 MPa), water is injected from one end of the slab. Due to the negative pressure environment, the water will be automatically sucked into the slab in the early stage, and the original formation will be formed under positive pressure (displacement pressure of 300 mbar) to displace in the later stage. In the water model, the duration of saturated water is 12 h

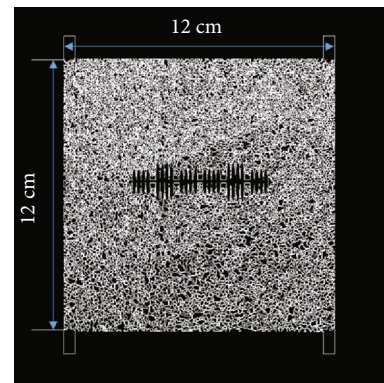


FIGURE 4: Design drawing of horizontal fracture lithography model in horizontal wells.

- (2) Saturated oil to bound water state, carry out oil flooding experiments on the models until only oil is produced but no water is produced. Full-view and partial image scanning and photographing are performed on each model, and the original oil saturation of each model is counted. The distribution of crude oil in the pores of reservoir rocks is controlled by the microscopic pore structure. Reservoir rocks with different pore types and pore sizes have different crude oil distribution patterns. Since the pore throats in the model are hydrophilic, a small amount of bound water will be formed on the pore walls. The viscosity and density of the selected experimental oil are similar to those of the crude oil to ensure the authenticity and credibility of the experimental results as much as possible (Figures 6(b) and 6(d))
- (3) Drive oil to the remaining oil state. After the crude oil and irreducible water models are established, the displacement experiment can be started. The experimental procedure is mainly to drive water, gas, and foam to the remaining oil to simulate the movement characteristics of the underground fluid during the development process. Images collected



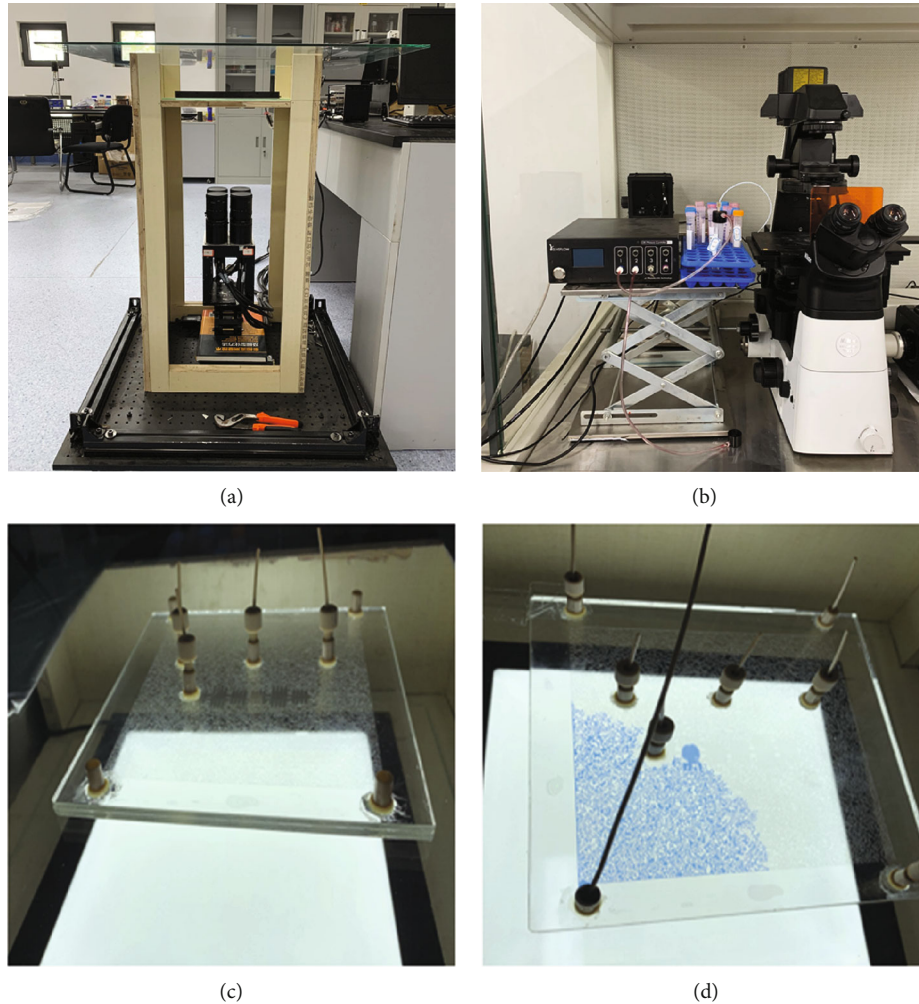


FIGURE 5: Visualized displacement experiment process: (a) image acquisition system; (b) pressure control system; (c) light source system; (d) model connection fluid line.

during the whole process of oil displacement under constant pressure (displacement pressure of 300 mbar) and constant temperature (room temperature of 23°C), the remaining oil saturation of the flat plate model is counted, and the oil displacement efficiency of different well types and displacement methods are calculated, as shown in Figure 7

## 5. Experimental Results and Discussion

**5.1. Analysis of Oil Displacement Effect.** Through the image pore processing software, the original porosity, saturated oil phase porosity, and oil phase porosity after displacement after the slab simulation of different well types and displacement methods are statistically calculated and the original oil saturation, remaining oil saturation, and oil displacement efficiency. The CIAS-2000 microscopic visual oil displacement image analysis system developed by the Institute of Image Information of Sichuan University was used to collect dynamic images and calculate the recovery factor. The results are shown in Table 1 (considering the actual control

range of horizontal wells, the quantitative analysis of remaining oil in horizontal wells adopts half of the model).

For conventional well types, the time consumed of water, nitrogen, and foam for the three media to drive to the remaining oil state is 352 minutes, 69 minutes, and 118 minutes, respectively. Due to the existence of horizontal fractures, the displacement takes effect quickly, the displacement is large, and it is easy to form a continuous flushing effect. At the same time, the layout of the three development wells is also easier to expand the swept volume. Nitrogen flooding and foam flooding have the best effects and the highest efficiency (swept area, oil displacement efficiency, and displacement time). Among them, nitrogen flooding has the best displacement effect around gas injection wells, and the remaining oil is mainly concentrated in the position between the development wells; the foam flooding effect is slightly poor, followed by water flooding. The water flooding method is uniformly displaced, the remaining oil is evenly distributed, and there is more remaining oil; the throughput efficiency is very low, and only local oil-water exchange occurs around the water injection well (Figures 7(a)–7(d)).

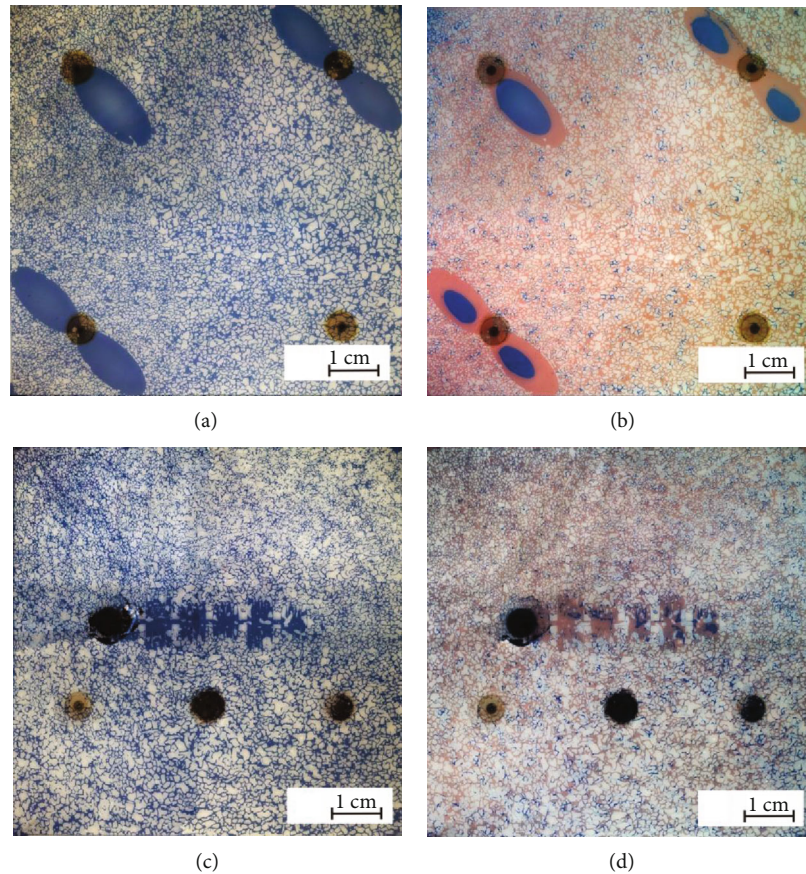


FIGURE 6: Full view of saturated water and oil on the flat panel (the blue area is water, and the red area is oil). (a) Full view of saturated water in horizontal fractured conventional wells. (b) Full view of saturated oil in horizontal fractured conventional wells. (c) Full view of saturated water in horizontal wells with horizontal fractures. (d) Full view of saturated oil in horizontal wells with horizontal fractures.

For the horizontal well type, it takes 164 minutes, 50 minutes, and 86 minutes to drive to the remaining oil state with water, nitrogen, and foam media, respectively. Nitrogen flooding has the best effect. It has the fastest effect near the injection well. There is little remaining oil within the control range of horizontal wells. The remaining oil is mainly concentrated at both ends of the horizontal well; water flooding has the lowest effect. When the water is injected, it takes effect between the injection wells soon. When the waterway is connected to the fracture, the remaining oil in the other untouched areas is slow to produce (Figures 8(e)–8(g)).

**5.2. Classification and Quantitative Analysis of Remaining Oil Occurrence Status.** Through the analysis and processing of the remaining oil distribution images, the microremaining oil can be divided into six categories according to the microremaining oil flow pattern, occurrence location, and oil-water contact relationship, combined with the classification standards of different types of microremaining oil established by the previous research: strip shape, mesh shape, column shape, island shape, plug shape, and membranous shape [4].

Because the mesh, strip, and column are essentially the combination of plug-like residual oil of different sizes and shapes, their force-bearing shapes are basically the same,

and the plug-like residual oil will eventually evolve into island-like residual oil or film-like residual oil, and according to the contact relationship between the remaining oil and the fluid and solid boundaries, as well as the analysis of its stress conditions, it shows that the remaining oil in the form of membranes is the most difficult to use, followed by islands and plugs, followed by columns, strips, and nets.[17, 18]

The image extraction process of microscopic remaining oil types using computer technology is skeleton extraction, pore throat central axis extraction and correction, pore throat segmentation, data correction, oil-water separation, and single-block remaining oil extraction. Figure 6 shows the remaining oil extraction results.

Analyzing the experimental parameters and displacement results (Figures 9(a)–9(c)), it is found that the foam flooding displacement efficiency is generally higher than the water flooding effect, but lower than the gas flooding effect; at the same time, the effect of conventional well type application is not much different from the gas flooding effect and is slightly worse than the gas flooding effect. The performance is not ideal in horizontal well types, and the displacement efficiency is only higher than the water drive effect, which is quite different from the gas drive effect.

By analyzing the microscopic remaining oil distribution state of different displacement methods, it can be found that



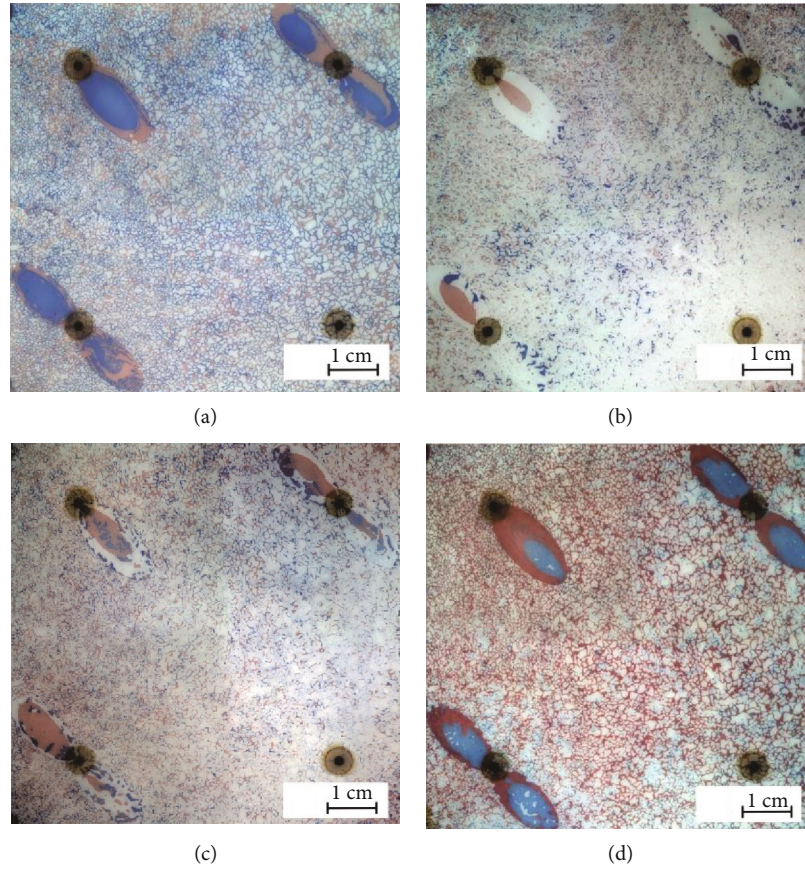


FIGURE 7: Comparison of effects of conventional wells with different development methods (the blue area is water, and the red area is oil): (a) water flooding; (b) nitrogen flooding; (c) foam flooding; (d) throughput.

TABLE 1: Displacement effect statistics of different well types.

Well type	Displacement method	Original porosity (%)	Saturated oil-water phase face ratio (%)	Saturated oil-oil phase face ratio (%)	Original oil saturation (%)	Oil phase face ratio after displacement (%)	Remaining oil saturation (%)	Oil displacement efficiency (%)
Horizontal fracture conventional well	Water	30.72	4.36	26.36	85.81	22.18	72.20	15.86
	Nitrogen	27.99	3.21	24.78	88.53	11.28	40.30	54.48
	Foam	28.46	3.32	25.14	88.33	12.59	44.24	49.92
	Throughput	27.56	4.80	22.76	82.58	21.58	78.30	5.18
Horizontal fracture horizontal well	Water	31.55	7.98	23.57	74.71	19.30	61.17	18.12
	Nitrogen	32.02	7.34	24.68	77.08	8.16	25.48	66.94
	Foam	30.92	7.97	22.95	74.22	10.90	35.25	52.51

in the water flooding method, since the matrix is hydrophilic, the injected water easily forms a water film on the pore walls and flows along the pore walls. The continuous columnar and large oil droplets scoured by the injected water will be cut off and displaced forward, but this will cause a large amount of remaining oil to be distributed in the middle of the pores and pores. Although the water flooding method is uniformly displaced and the affected area is large, the remaining oil saturation is high [19–21]. The

remaining oil of gas flooding and foam flooding mostly exists in the corners of pores and small pores. Most of the remaining oil forms are in the form of plugs and columns, and there is no continuous network and stripes after water flooding, remaining oil distributed in strips.

For the morphological distribution of the extracted single piece of remaining oil, the image feature parameters such as shape factor, circularity, concavity, aspect ratio, Euler number, contact ratio, and the number of pore throats

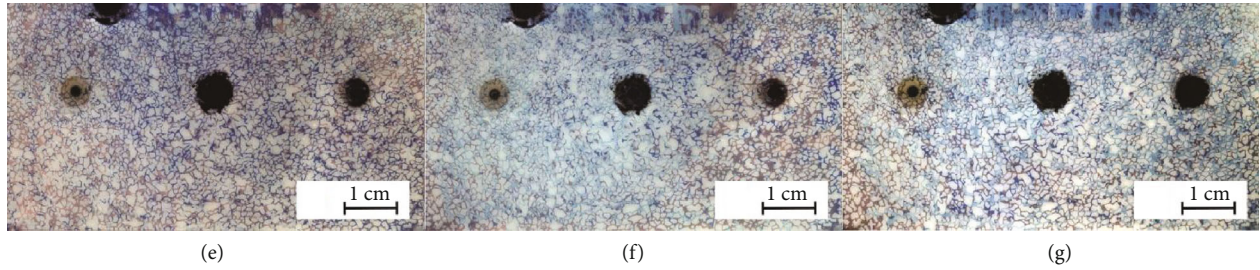
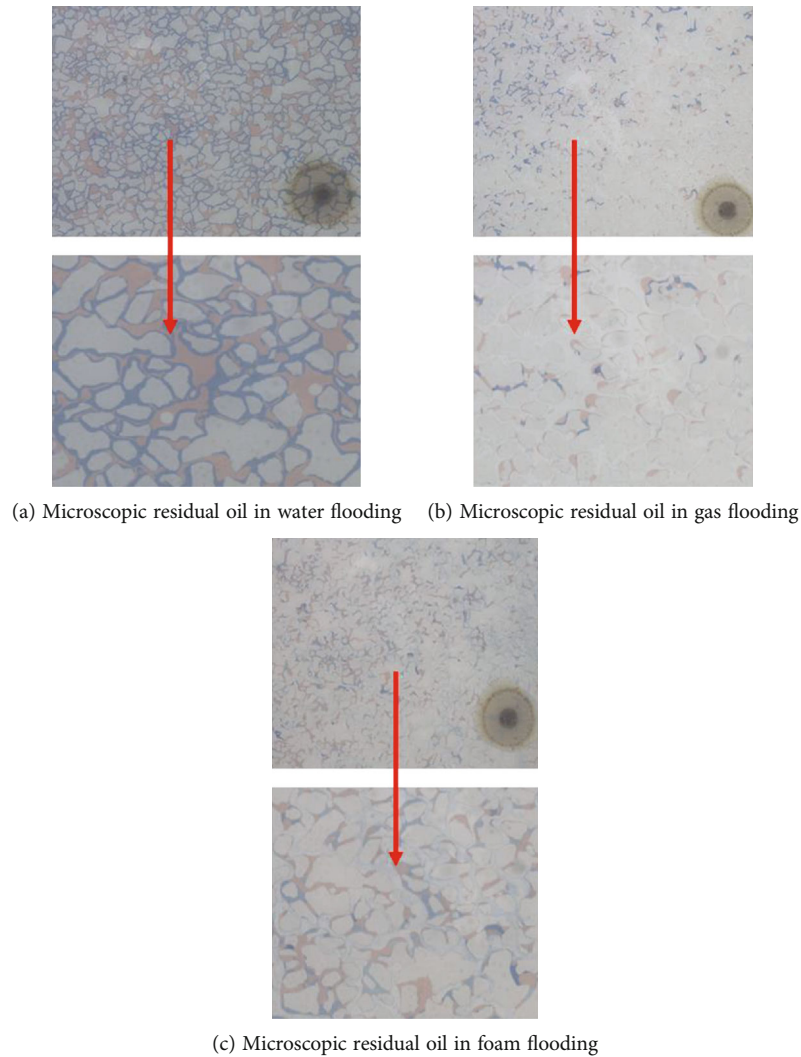


FIGURE 8: Comparison of effects of horizontal wells with different development methods (the blue area is water, and the red area is oil): (e) water flooding; (f) nitrogen flooding; (g) foam flooding.



(a) Microscopic residual oil in water flooding (b) Microscopic residual oil in gas flooding

(c) Microscopic residual oil in foam flooding

FIGURE 9: Microscopic residual oil occurrence states of different displacement methods (the blue area is water, and the red area is oil).

occupied are selected according to different remaining oil classifications. For the extraction and description of graphic features, the number and area percentages of various types of microscopic remaining oil after the end of different displacement methods are shown in Tables 2 and 3.

The remaining oil face ratio and remaining oil form area ratio calculated by different displacement media are treated

uniformly. From the results (Table 3), the effect of gas flooding and foam flooding in conventional well types is better than that of water flooding and water flooding remaining oil. The morphology is mainly striped and networked. The main reason for the large remaining oil is that there is still a large number of contiguous remaining oil that has not been used; the residual oil of gas flooding and foam flooding

TABLE 2: Analysis data table of remaining oil form number ratio.

Number: microfluidic flat panel model Picture number	Software version: CIAS-2000					
	Mesh	Striped	Columnar	Plug	Isolated island	Membranous
Ratio of remaining oil formed in conventional well water flooding (%)	8.00	10.92	42.56	15.07	20.06	3.39
Ratio of remaining oil forms in conventional well foam flooding (%)	2.18	3.36	54.83	11.34	26.62	1.68
Ratio of remaining oil forms in conventional well gas flooding (%)	1.48	2.79	54.36	9.16	30.54	1.66
Ratio of remaining oil forms in horizontal well foam flooding (%)	10.94	18.06	43.06	20.83	4.86	2.26
Ratio of remaining oil forms in horizontal well gas flooding (%)	6.71	12.50	46.95	25.30	4.27	4.27
Ratio of remaining oil forms in horizontal well water drive (%)	6.85	5.84	51.44	12.06	20.00	3.81

TABLE 3: Analysis data table of remaining oil form area ratio.

Number: microfluidic flat panel model Picture number	Software version: CIAS-2000					
	Mesh	Striped	Columnar	Plug	Isolated island	Membranous
Remaining oil form area ratio of conventional well water flooding (%)	5.60	9.60	3.38	2.58	0.53	0.50
Conventional well gas flooding remaining oil form area ratio (%)	0.62	1.64	5.37	1.70	1.55	0.41
Foam flooding remaining oil form area ratio of conventional wells (%)	1.49	1.67	5.48	2.16	1.33	0.46
Remaining oil form area ratio of horizontal well water drive (%)	4.60	3.63	6.25	2.66	1.11	1.05
Remaining oil form area ratio of horizontal well gas flooding (%)	0.73	6.50	0.54	0.32	0.04	0.04
Remaining oil form area ratio of horizontal well foam flooding (%)	2.38	4.58	2.20	1.42	0.16	0.16

is mainly columnar and striped, which can be seen. In conventional well types, water flooding has a good effect on the remaining oil in columnar and island shapes. Gas flooding has a good effect on the remaining oil in net, plug, and film. Strip-like remaining oil has a good effect.

The gas flooding effect in horizontal well type is also better than foam flooding and water flooding. The remaining oil in water flooding is mainly columnar and network. Among them, water flooding has a good effect on the remaining oil in strips; the overall effect of gas flooding is better and the remaining oil. The oil is mainly strip-shaped, and the remaining oil in other forms is very small, especially for island-shaped and film-shaped remaining oil. The remaining oil in foam flooding is mainly strip-shaped and network-shaped, and the remaining oil forms are distributed, but the overall amount is small [22–25].

## 6. Conclusions

Based on the microfluidic flat plate model experiment, this paper discusses the microresidue comprehensively for specific development well patterns (inverse seven-point well patterns), well types, and fracture occurrence patterns (horizontal fractures) generated by fracturing, taking into account the comparative displacement methods, the law of effective use of oil.

- (1) The net-like, strip-like, and column-like patterns of microscopic remaining oil are essentially a combination of plug-like remaining oil of different sizes and shapes. The plug-like remaining oil will eventually evolve into island or film-like remaining oil, plug-like remaining oil production mechanism in order to increase the

displacement pressure difference; the membrane-like remaining oil production mechanism is to change the interfacial tension and increase the mobility ratio; the island-like remaining oil production mechanism is to increase the mobility ratio; the difficulty of the remaining oil production in actual production ranges from mesh to the film-like difficulty which increases successively

- (2) The effect of nitrogen flooding and foam flooding in horizontal fractured conventional well types is better than that of water flooding. After nitrogen flooding and foam flooding, the remaining oil forms are mainly columnar and plug. The remaining oil saturation is high (72.2%). The main reason for this type of remaining oil is that there is still a large amount of contiguous remaining oil that has not been used
- (3) Horizontal wells with horizontal fractures have the best nitrogen flooding effect. The remaining oil saturation is low (25.48%). After nitrogen flooding, the remaining oil is mainly striped, and the remaining oil content of other types is low; remaining after water flooding. The oil form is mainly columnar and reticulated; the remaining oil form after foam flooding is mainly striped and reticulated
- (4) It is recommended that conventional well horizontal fracture reservoirs adopt nitrogen flooding/foam-driven water injection to develop the remaining oil or directly adopt nitrogen flooding/foam flooding in the early stage; for horizontal wells and horizontal fracture reservoirs, nitrogen-driven water injection development should be used. The remaining oil formed later may be directly developed by nitrogen flooding



## Data Availability

All data generated or analyzed during this study are included in this article.

## Conflicts of Interest

The authors declare that the paper does not have any conflict of interest with other units and individuals.

## Acknowledgments

The authors acknowledge the financials—project (2019JQ-151) supported by the Natural Science Foundation Research Project of Shaanxi Province and project (JZ2021HGQB0284) supported by the Fundamental Research Funds for the Central Universities.

## References

- [1] F. W. Yu, Z. D. Gao, W. H. Zhu et al., “Experiments on the seepage mechanism of fractured reservoirs based on microfluidic model,” *Petroleum Exploration and Development*, vol. 48, no. 5, pp. 1162–1172, 2021.
- [2] C. Wang, H. Q. Jiang, M. Q. Ma, F. W. Yu, Y. Y. Zhao, and J. J. Li, “Research on pore-scale remaining oil flow state change law based on microfluidic model,” *Petroleum Science Bulletin*, vol. 5, no. 3, 2020.
- [3] J. H. Shen, “Study on the seepage characteristics of microscopic remaining oil in the ultra-high water-cut stage of water-flooding reservoirs,” *China Chemical Industry Trade*, vol. 010, no. 003, 2018.
- [4] S. W. Ding, H. Q. Jiang, and X. Yi, “Micromechanical causes and channel selection mechanism of remaining oil in ultra-high water cut period,” *Journal of Liaoning University of Petroleum & Chemical Technology*, vol. 38, no. 1, 2018.
- [5] B. Bo, S. Jiawei, F. Jia, Y. Zaiyong, P. Baoliang, and Z. Shuangliang, “Research progress of surfactant-enhanced oil displacement based on microfluidic technology,” *Chinese Journal of Petroleum*, vol. 43, no. 3, pp. 432–442, 2022.
- [6] N. K. Karadimitriou and S. M. Hassanizadeh, “A review of micromodels and their use in two-phase flow studies,” *Vadose Zone Journal*, vol. 11, no. 3, pp. 215–228, 2012.
- [7] B. Chen, *Diagenesis differences and productivity evaluation of low-permeability sandstone reservoirs*, Northwest University, 2020.
- [8] K. Yang and S. Y. Xu, “Research on microscopic remaining oil experimental method,” *Fault Block Oil & Gas Field*, vol. 16, no. 4, 2009.
- [9] Y. Liang, Q. M. Gan, C. Zhao, S. Fan, H. X. Shi, and Y. Lei, “The whole life cycle benefit evaluation of pumping unit based on AHP,” *Petroleum and Petrochemical Energy Conservation*, vol. 9, no. 4, 2019.
- [10] L. H. Wang, H. F. Xia, P. H. Han, R. B. Cao, X. D. Sun, and S. Q. Zhang, “The microscopic characteristics of the remaining oil distribution and the quantitative characterization of its availability,” *Litologic Reservoirs*, vol. 33, no. 2, pp. 147–154, 2021.
- [11] B. Ding, C. M. Xiong, X. F. Geng et al., “Characteristics and EOR mechanisms of nanofluids permeation flooding for tight oil,” *Petroleum Exploration and Development*, vol. 47, no. 4, pp. 810–819, 2020.
- [12] J. J. Li, Y. Liu, Y. J. Gao, B. Y. F. Cheng, F. Meng, and H. Xu, “The effect of microscopic pore-throat heterogeneity on the distribution of remaining oil,” *Petroleum Exploration and Development*, vol. 45, no. 6, pp. 1043–1052, 2018.
- [13] X. Y. Gu, C. S. Pu, H. Huang et al., “Micro-influencing mechanism of permeability on spontaneous imbibition recovery for tight sandstone reservoirs,” *Petroleum Exploration and Development*, vol. 44, no. 6, pp. 1003–1009, 2017.
- [14] L. Chen, *Study on the Start-Up Conditions of Microscopic Remaining Oil and the Mechanism of Oil Film Deformation in the Ultra-High Water Cut Period*, Southwest Petroleum University, 2017.
- [15] B. Chen, *Characteristics and Productivity Analysis of Low Permeability Reservoirs in Ordos Basin*, Northwest University, 2016.
- [16] W. C. Yan and J. M. Sun, “Analysis of the status quo of microscopic remaining oil research,” *Progress in Geophysics*, vol. 5, 2016.
- [17] W. J. Wang, *Fabrication of Microfluidic Chip and Its Application in Analysis*, Fuzhou University, 2010.
- [18] J. Wang, J. Hou, Y. T. Qu, F. M. Gong, and F. Li, *Microscopic Distribution Image of Remaining Oil in Porous Media Collection and quantitative characterization methods*, Beijing, 2016, CN104076046B.
- [19] P. Wu, *Research on the Micro-Displacement and Seepage Characteristics of High Water-Cut Oil Reservoirs and the Improvement of Remaining Oil Recovery*, China University of Geosciences, Beijing, 2014.
- [20] Y. Liang, H. X. Shi, W. Wei, C. Zhao, and S. Fan, “Research on effective production technology of remaining oil in mid-high water cut period in Ansai Oilfield,” *Petroleum Geology and Engineering*, vol. 28, no. 6, 2014.
- [21] X. Y. Ku, *Research on the Rapid and Low-Cost Manufacturing Process of Prototype Microfluidic Chips*, Chongqing University, 2019.
- [22] Q. Xu, *Evaluation of Production Status and Production Measures of Thin-Poor Reservoirs in High Water Cut Period*, Northeast Petroleum University, 2019.
- [23] R. Lenormand, E. Touboul, and C. Zarcone, “Numerical models and experiments on immiscible displacements in porous media,” *Journal of Fluid Mechanics*, vol. 189, no. 189, pp. 165–187, 1988.
- [24] C. Wang, H. Jiang, J. Liu, L. Mi, and J. Li, “An advanced approach to study the seepage characteristics of dynamic remaining oil in porous media at pore scale,” in *79th EAGE Conference and Exhibition 2017 - SPE EUROPEC*, Paris, France, 2017.
- [25] L. Mi, H. Jiang, Y. Pei et al., “Microscopic oil and water percolation characteristic investigation of water flood reservoir in ultrahigh water cut period,” in *SPE Trinidad and Tobago Section Energy Resources Conference*, Port of Spain, Trinidad and Tobago, 2016.